IPPI
Polyolefins Journal, Vol. 1 No. 2 (2014) 117-129
ORIGINAL PAPER

The role of 1-hexene comonomer content in thermal behavior of medium density polyethylene (MDPE) synthesized using Phillips catalyst

Abbas Kebritchi[1,2], Mehdi Nekoomansh[1*], Fereidoon Mohammadi[1], Hossein Ali Khonakdar[2]

[1]Iran Polymer and Petrochemical Institute, 14965-115, Tehran, Iran

[2]Leibniz Institute of Polymer Research, D-01067 Dresden, Germany

Received: 9 July 2014, Accepted: 1 Septermber 2014

ABSTRACT

In this work, the role of comonomer content of 1-hexene-medium density polyethylene (MDPE) copolymer, synthesized using Phillips catalyst, on thermal behavior parameters such as: crystallization, melting temperature and thermal degradation was investigated in detail. The copolymer was fractionated to homogenous short-chain branching (SCB) fractions by "preparative temperature rising elution fractionation" (P-TREF) method and then it was subjected to thermal analyses. A broad chemical composition distribution (CCD) in terms of SCB content and molecular weight (M_w) was observed by P-TREF and gel permeation chromatography (GPC), respectively. Based on P-TREF results, a parabolic relationship between methylene sequence length (MSL) and elution temperature (ET) was presented. Differential scanning calorimetry (DSC) showed distinct, well-defined melting peaks over a 22 °C temperature range for SCB contents of about 3-12 (br/1000 C). The variations in physical characteristics such as melting temperature (T_m), crystallinity (X_c), crystallization temperature (T_c) and lamellae thickness (L_c) against SCB content were correlated. Thermogravimetric analysis (TGA) suggested linear relationships between the temperature at maximum degradation rate (T_{max}) as well as the degradation initiation temperature ($T_{5\%}$) versus SCB content. Moreover, the TGA curves exhibited distinct differences at both initiation and propagation stages of thermal degradation at dissimilar comonomer contents. **Polyolefins J (2014) 1: 117-129**

Keywords: ethylene/1-hexene copolymer, short-chain branching (SCB), thermal degradation, Phillips catalyst, medium density polyethylene (MDPE)

INTRODUCTION

Polyethylene (PE), the most important member of polyolefins family [1, 2], is frequently used for agricultural film purposes such as greenhouse, mulching, tunnel film, etc. [3]. The frequent use of PE is due to its convenient properties such as low cost, easy processability, excellent electrical insulation, chemical resistance, toughness, flexibility, transparency in thin films and freedom from odor and toxicity [4, 5]. Linear PEs are produced by the copolymerization of ethylene and α-olefins, e.g., 1-butene, 1-hexene and 1-octene, with either Ziegler–Natta (Z-N), metallocene, Phillips or other catalysts [6]. It is well known that heterogeneous Z–N catalysts polymerize ethylene/α-olefin copolymers with a broad chemical composition distribution (CCD) [7-9]. In contrast, homogeneous metallocenes are single-site catalysts which produce very uniform polymers with a narrow CCD [10-13]. However, there

* Corresponding Author - E-mail: m.nekoomanesh@ippi.ac.ir

is hardly any report on the role of Phillips catalyst on the microstructure of ethylene/α-olefin copolymers [14-16].

Specifications of the catalyst, reactor processing technology and conditions of the manufacturing process mainly configure the microstructure of PEs. Resins of similar densities might exhibit significant differences in comonomer content and its distribution, at both the intermolecular and intramolecular levels [17]. Besides, molecular structure parameters including molecular weight (M_w) and molecular weight distribution (MWD), branching parameters including branch content, branch length, and branch distribution will normally determine the ultimate property of PE [18]. The SCB content and the short-chain branching distribution (SCBD) of an ethylene/α-olefin copolymer are key microstructural constraints that determine resin performance and applications [19-21].

There are many reports in the literature which investigate the relationship between structure and properties of PEs, e.g., the effect of chemical modification on crystallization [22], the role of branching structure on melting behavior [23] as well as melt flow index [24], the influence of branch length on mechanical properties [25], the effect of composition distribution on miscibility of the blends [26] and the dependency of thermorheological behavior on molecular structure [27]. Hosoda et al. have investigated a relationship between the lamellae thickness distribution and the mechanical properties of PE. They observed a higher impact strength at narrower lamella thickness distribution [28]. Also Nittaa and Tanaka have illustrated that both SCB content and molecular weight of ethylene-1-hexene polymers affect both the α and β relaxation peaks [29].

Different studies show that the CCD of polyethylenes has some important effects on thermal properties [30-33]. Stark and Lofgren have worked on DSC of metallocene type copolymers of ethylene with 1-octene, 1-tetradecene and 1-octadecene. They suggested that the melting temperature is dropped by increasing the comonomer content [34]. Eynde et al. have reported that thermal behavior of copolymers change in a continuous way as the comonomer content is increased [35]. Zhang et al. have studied on melting and crystallization of "preparative temperature rising elution fractionation" (P-TREF) fractions of two different polymers. They proposed that the melting and crystallization temperatures and enthalpy of fusion (ΔH_f) of the P-TREF fractions for a Z-N polymer are substantially decreased by comonomer content, while these properties are varied slightly for a metallocene polymer [36]. Ko YS et al. have stated that the physical properties of α-olefin copolymers are dependent on distribution of the comonomer as well as on the molecular weight [7]. Grieken et al. have accounted that by increasing the short branching coming from the incorporation of α–olefins of low melting points, crystallinity and density would consequently result in more flexible films which will be easier to process [10].

There are various research reports in the literature which have been focused on degradation of linear polyethylenes under different conditions such as ultraviolet (UV) irradiation [37]; extrusion [38]; thermo-oxidation [39, 40]; thermo [41]; artificial weathering [42] and environmental weathering [43]. They have to a large extent focused on the parameters of thermal degradation process, e.g., the effects of operational parameters [44-46] and catalyst parameters [47-50]. However, to the best of our knowledge there is hardly any study on the effect of "polymer architecture" on the thermal degradation behavior [51, 52]. Now the question would be if the comonomer content affects the thermal degradation behavior of polyethylene copolymers?

In our previous works the effect of molecular weight [44, 53, 54] as well as the effect of ethyl branch content [55] on thermal degradation of polyolefins was investigated in depth. In this study the effect of comonomer content on thermal behavior of ethylene/1-hexene copolymer based on Phillips catalyst is examined. To study accurately and to eliminate any other microstructural parameters, the ethylene/1-hexene copolymer (MDPE) was fractionated to homogenous SCB content fractions using P-TREF technique. The role of SCB content on crystallization, melting and especially thermal degradation of each fraction was investigated in order to find any functionality between the thermal behavior and the comonomer content of Phillips-based ethylene/1-hexene copolymer.

EXPERIMENTAL

Material

"Parent polymer" was an industrial grade of MDPE (MCH 3713, synthesized based on a special Philips catalyst, Aryasasol Petrochemical Company, Iran) which was an ethylene copolymer with 1-hexene as comonomer (Table 1).

Preparative temperature rising elution fractionation

The home-made P-TREF consisted of a cylindrical column 7 cm in diameter and 40 cm in height. This column was packed with seeds of an average diameter of 0.07 cm and submerged in an oil bath with a programmable thermostat that controlled the temperature of the bath. In each run a polymer solution with concentration of 1 wt% of parent polymer in xylene was introduced into the column and heated at 140°C for 2 h and then cooled to room temperature (30°C) slowly at a rate of -3°C/h to crystallize the parent polymer chains on the seeds. The bath temperature was subsequently increased and maintained for about 2 h at each elution temperature (ET) to elute the polymer chains of specific crystallizability completely by a stream of pure solvent (xylene). After dissolution of polymer chains, the fractions in solvent steam were treated with anti-solvent (acetone) to separate and precipitate the polymer fractions. After separation, the prepared fractions were tested by subsequent tests including DSC and TGA.

Structural analysis

Fourier transform infrared (FTIR) spectrometer (Vertex 80, Bruker, Germany) was used to characterize the parent polymer structure. The attenuated total reflectance (ATR) spectra were recorded in the range of 4000–600 cm^{-1}, 100 scans each measurement with resolution of 2 cm^{-1} using MCT detector.

Proton nuclear magnetic resonance (^{1}H NMR) spectra were recorded on a Bruker DRX 500 spectrometer operating at 500.13MHz for ^{1}H NMR. $C_2D_2Cl_4$ was employed as the solvent at 120°C. The spectra were referenced on the residual C_2HDCl_4 signal δ (1H) = 5.98 ppm. The butyl branch content of parent polymer was calculated based on ^{1}H NMR signal integrals from the integral intensities of methyl protons which originated from hexyl comonomer (0.92 ppm) and of all methine and methylene protons (1.1 – 1.8 ppm) with estimated absolute error: ± 0.5 mol%.

M_w and MWD of the parent polymer and P-TREF fractions were determined by means of gel permeation chromatography (GPC, PL_GPC of Polymer Laboratories, Agilent, USA) using 1,2,4 trichlorobenzene (TCB) as solvent at separating column of 300×7.5 mm (2 PLgel_Olexies) with flow velocity of 1.0 mL/min at the temperature of 150 °C.

Table 1. Specifications of the parent polymer.

Property	Test method	Typical value	Reference
Melting point (°C)	ISO 3146	125.3	Measured
Melt flow index (MFI) (190 °C/2.16 kg) (g/10 min)	ISO 1133	0.16 ±0.01	Datasheet
Melt flow index (MFI) (190 °C/21.6 kg) (g/10 min)	ISO 1133	17.01±0.01	Datasheet
Density (g/cm^3)	ISO 1183	0.935	Datasheet
Butyl branch content (mol%)	^{1}H NMR	1.2	Measured

Low/high temperature thermal analyses

Thermograms of parent polymer and P-TREF fractions were assessed by a Mettler differential scanning calorimetry (DSC) (Toledo, Switzerland) under N_2 atmosphere, in which the samples were heated fast (200°C/min) to 180 °C and maintained at this temperature for 5 min to erase any thermal history, and then cooled to room temperature (30°C) at a rate of -10°C/min. This was immediately followed by a second heating run (10°C/min) in order to detect a complete melting behavior of the samples.

The thermogravimetric analysis (TGA) of parent polymer and P-TREF fractions was made using TGA Q 5000 of TA Instruments, under N_2 atmosphere. The fractions experienced an isothermal condition for 5 min at room temperature and then heated up with a ramp at 10°C/min to 600 °C.

RESULTS AND DISCUSSION

Characterization of parent polymer and fractions

The structural characterization of the parent polymer

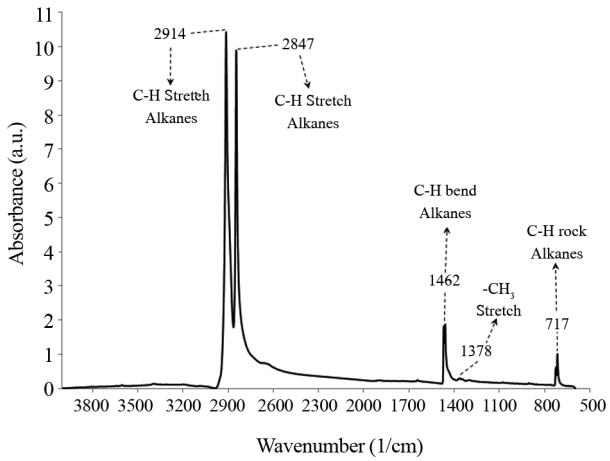

Figure 1. FTIR spectrum of the parent polymer

was prepared by FTIR as shown in Figure 1. The C-H rocking, methyl stretching, C-H bending and stretching at 717, 1378, 1462, 2847 and 2914 cm^{-1} wavenumbers; respectively, gave indications of a common structure of PE [56]. Butyl branch content of the parent polymer was calculated based on ^{1}H NMR and presented in Table 1.

Mw and MWD of the parent polymer and P-TREF fractions are shown in Figure 2 and a quantitative comparison of the results is reflected in Table 2. As it is noticed in Table 2, a broad MWD (≈7.3) for the parent polymer is obtained. Also, as it can be found in section of "Investigation on comonomer distribution", a broad short-chain branch distribution (SCBD≈1.2) has been calculated based on Eqn 6. Both of the obtained distributions are in a good agreement with previous research reports which propose a broad CCD for Phillips based ethylene copolymers [14-16]. Also, as it can be seen in Table 2, in an agreement with the literature [57, 58], by rising the fraction temperature (lowering the SCB content), the molecular weight is increased except that for 60-70 fraction, though a narrow MWD can be more or less observed for the fractions.

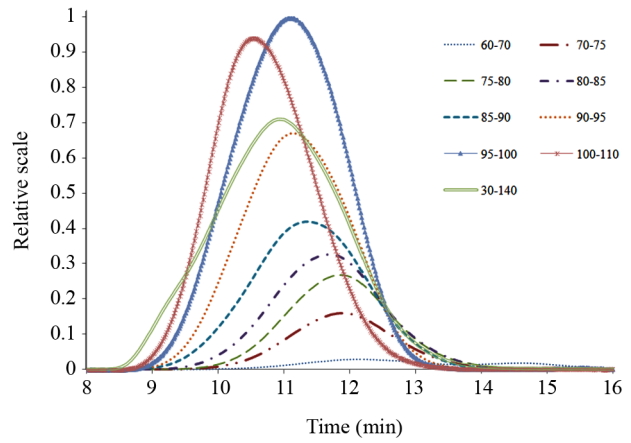

Figure 2. Molecular weight distribution for the parent MDPE and P-TREF fractions

Table 2 SEC-MALLS obtained data for parent polymer and the P-TREF fractions.

Fraction	M_n (g/mol)	M_w (g/mol)	MWD
60-70	40,000	55,000	1.4
70-75	14,000	46,000	3.3
75-80	15,000	53,000	3.5
80-85	18,000	64,000	3.6
85-90	30,000	104,000	3.5
90-95	55,000	159,000	2.9
95-100	106,000	259,000	2.4
100-110	112,000	379,000	3.4
Parent polymer	26,000	190,000	7.3

Investigation on comonomer distribution

Figure 3 represents accumulative P-TREF profile of the parent polymer, which intonates a broad SCBD. Phillips catalysts cause heterogeneity in short-chain branched polyethylenes [14-16], this broad SCBD may be attributed to Phillips catalyst function during polymerization. Also, methylene sequence length (MSL) of the fractions is plotted versus elution temperature (ET) in Figure 3.

Zhang and Wanke have shown that MSL as a func-

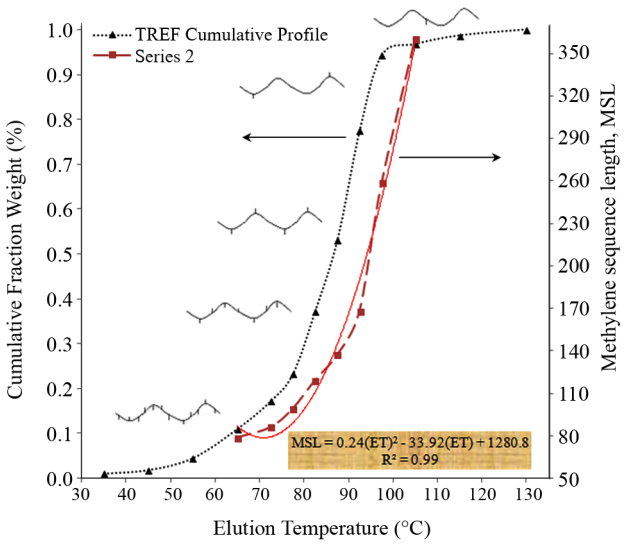

Figure 3. P-TREF cumulative profile of the parent polymer and MSL variations of the fractions versus elution temperature.

tion of the melting temperature (T_m), in K can be estimated by a calibration correlation, using Eqn 1 [59]:

$$MSL = \frac{2}{\exp\left(\frac{142.2}{T_m} - 0.3451\right) - 1} \quad (1)$$

As it may be studied in Figure 3, by rising ET the MSL of the fractions is increased from about 79, at the most branched fractions, up to around 360 at the most linear fractions. A parabolic relationship is yielded between MSL and ET with regression coefficient of $R^2 \approx 0.99$ which is valid in the range of 60°C < ET< 110 °C and can be predicted by Eqn 2:

$$MSL=0.24\times(ET)2-33.92\times(ET)+1281 \quad (2)$$

Kakugo et al. have reported that ethylene content of different fractions of ethylene/1-hexene copolymer is increased by increase in elution temperature [60]. Adisson et al. have found that by increasing SCB content elution temperature is decreased for ethylene/1-hexene copolymer through a linear correlation [61].

By counting the carbon atoms and CH_3 groups for the 'repeating unit' in an ethylene/α-olefin molecule with the same methylene sequence length and neglecting the effect of end groups, the short-chain branch (SCB) content, per 1000 carbons, as a function of MSL can be estimated by Eqn 3 [59], where i is the carbon number in the branch (e.g., for 1-hexene comonomer i is 4).

$$SCB = \frac{1000}{MSL + i + 1} \quad (3)$$

The number average short-chain branch content, $\overline{SCB_n}$, and weight average short-chain branch content, $\overline{SCB_w}$, might be calculated based on the first and second moments of the SCB distributions, similar to the number and weight average molecular weight distributions, according to Eqns 4 and 5:

$$\overline{SCB_n} = \sum_{i=1}^{n} w_i \times SCB_i \quad (4)$$

$$\overline{SCB_w} = \frac{\sum_{i=1}^{n} w_i \times SCB_i^2}{\sum_{i=1}^{n} w_i \times SCB_i} \quad (5)$$

Where wi is the mass fraction of fraction i (obtained from P-TREF results); SCBi is the SCB content of fraction i (calculated based on Eqn 3) and n is the number of fractions (here; n= 8, section of "The role of comonomer content on melting temperature and crystallization behavior"). Using Eqns 4 and 5, and are yielded around 6.4 and 7.8, respectively. Also in a similar way for calculation of MWD, the SCBD can be calculated, using Eqn 6:

$$SCBD = \frac{\overline{SCB_w}}{\overline{SCB_n}} \quad (6)$$

The amount of SCBD has been calculated around 1.2. In comparison to the literature [59, 62], the obtained SCBD value can be assumed as a broad SCBD.

The role of comonomer content on melting temperature and crystallization behavior

DSC thermograms of the second heating cycle and the melting temperatures of P-TREF fractions are presented in Figure 4, while the detailed information is tabulated in Table 3. Due to small amount of some fractions, acquired at 30-40°C, 40-50°C, 50-60°C, 110-120°C and 120-140°C, the thermal analysis of the samples is limited to the fractions mentioned in Table 3. In Figure 4, a fine confirmation on distinctive separation of P-TREF fractions can be detected as complete segregated melting peaks.

Approximately a wide temperature range (~22°C) from ~111°C up to ~132°C for melting peaks is observed alongside different fractions due to heterogeneity in SCB content. A broad melting temperature range for 1-hexene-linear low density polyethylene (LLDPE) and also a similar trend for variations in T_m versus SCB content have been reported for ethylene/1-

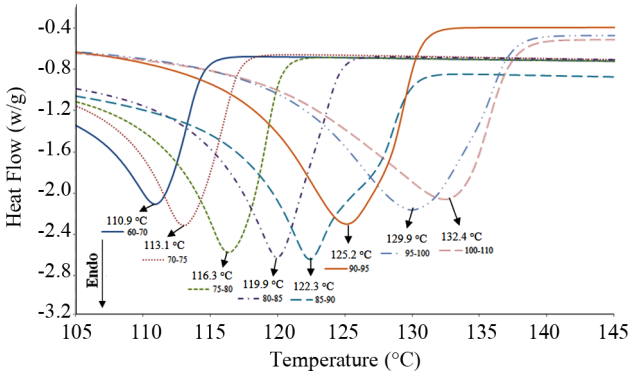

Figure 4. DSC thermograms of second heating cycle and melting temperatures for P-TREF fractions.

Figure 3. Detailed DSC data and the calculated parameters of P-TREF fractions.

Fraction	T_c[1] (°C)	T_m[2] (°C)	SCB[3] (br/1000 C)	L_c[4] (nm)	X_c[5] (%)	MSL[6]
60-70	100.2	110.9	11.9	6.6	38.2	78.5
70-75	101.6	113.1	11.0	7.1	41.0	85.8
75-80	104.9	116.3	9.6	8.0	47.1	98.9
80-85	108.4	119.9	8.1	9.4	45.7	118.9
85-90	110.9	122.3	7.0	10.6	52.4	137.0
90-95	111.1	125.2	5.8	12.5	50.2	167.5
95-100	111.2	129.9	3.8	17.6	50.2	258.4
100-110	110.9	132.4	2.7	22.5	51.2	360.3
30-140 (parent polymer)	114.5	125.3	5.8	12.6	46.6	168.7

[1]T_c: Crystallization temperature.

[2]T_m: Melting temperature.

[3]SCB: Short chain branch content calculated by Eqns 1 and 3.

[4]L_c: Lamellae thickness calculated by Gibbs-Thomson relationship Eqn 8.

[5]X_c: Crystallinity calculated by Eqn 9.

[6]MSL: Methylene sequence length calculated by Eqn 1.

hexene copolymer in the literature [61, 63].

Table 3 Detailed DSC data and the calculated parameters of P-TREF fractions.

Considering data in Table 3, a relationship between T_m and SCB content can be derived which is presented in Eqn 7 with regression coefficient of $R_2 \approx 1$. The Eqn 7 is analogous to Hosoda equation ($T_m = -1.69 \times (SCB) + 133$) for Z-N catalyst based 1-hexene-PE [62].

$$T_m\,(°C) = -2.3 \times (SCB) + 138.7 \quad (7)$$

The Eqn 7 has small variations from Hosoda equation especially at SCB coefficient which determines the sensitivity of Tm to SCB content [36]. In an agreement with the obtained results, Yoon et al. have worked on melting behavior of different ethylene/α-olefin copolymers synthesized by Z-N catalyst. They reported that the melting peak moves to a lower temperature regions as the density of the copolymers is decreased [64]. According to the Gibbs–Thomson equation (Eqn 8), it is possible to determine the lamellar thickness of different lamellae [24, 65-67]:

$$T_m = T_{0m} - \frac{1 - 2\,\delta e}{\Delta H \times L_c} \quad (8)$$

Where T_m (K) is the observed melting point, T_{0m}(K) is the equilibrium melting point of an infinite polyethylene crystal (414.5 K), ΔH is the enthalpy of fusion per unit volume (288×106 J/m^3), δe is the surface energy of a polyethylene crystal (70×10^{-3} J/m^2) and L_c (nm) is the thickness of a lamellae with melting point of T_m [28]. Also the crystallinity of each fraction can be calculated using Eqn 9:

$$X_c(\%) = \frac{\Delta H_f}{\Delta H_f^*} \times 100 \quad (9)$$

Where ΔH_f is the enthalpy of fusion of each fraction and ΔH_f^* is the enthalpy of fusion of 100% crystalline polyethylene (286 J/g) [68]. In Figure 5, SCB content and T_m are plotted against Lc. Based on these observations, Eqn 10 for predicting the reduction of SCB content versus lamellae thickness, exponentially and Eqn 11 for estimating the increases in melting point against lamellae thickness, logarithmically are proposed. Pérez et al. have studied on branched polyethylenes and showed that peaks in the end of endotherm thermograms may be associated to lamellae crystals formed by the crystallization of longer methylene sequences [69]. Also, Zhang et al. have reported similar trends for variations in SCB content versus L_c and also MSL against L_c [36]. Nitta and Tanaka [29] have studied on the mechanical behavior of branched polyethylene with different SCB contents. They reported similar trend for reduction of L_c with SCB content.

$$SCB = -6.7 \times \mathrm{Ln}\,(L_c) + 26.2 \quad (10)$$

$$T_m = 16.1 \times \mathrm{Ln}\,(L_c) + 80.3 \quad (11)$$

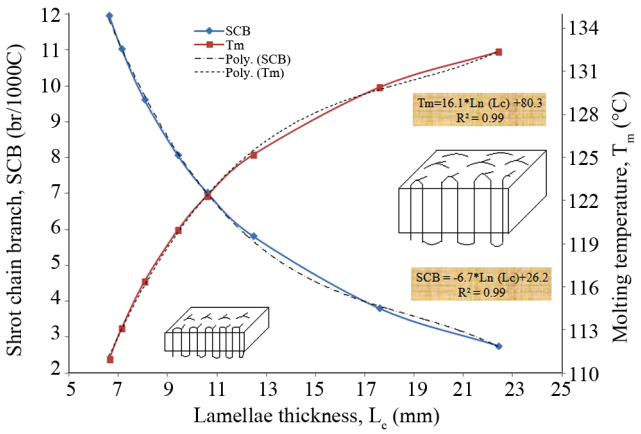

Figure 5. SCB content and T_m versus lamellar thickness of P-TREF fractions.

Where SCB, L_c and T_m are calculated in br/1000 C, nm and °C, respectively.

In Figure 6, crystallization temperature (T_c) and crystallinity have been plotted versus SCB content. As it can be viewed, both the T_c and X_c are decreased by SCB content. But, the interesting point is a two-stage behavior. The Figure 6 can be divided into two sections: section (1): SCB < 7.0 and section (2): SCB > 7.0. In section (1) of Figure 6 a constant amount for T_c and also a weak fluctuation around a constant value for X_c can be observed, it means that the crystallization temperature for SCB contents lower than 7.0 is independent of branching content. But, in section (2) of Figure 6 a decreasing trend for both X_c and T_c is visible which can be presented by Eqns 12 and 13.

$$T_c = -2.2 \times (SCB) + 126.2 \quad (12)$$

$$X_c = -2.5 \times (SCB) + 68.9 \quad (13)$$

Where T_c, X_c and SCB are considered in °C, % and br/1000 C.

The section (2) of Figure 6 is usually reported in previous studies. Paredes et al. have shown that by increasing the content of 1-hexene comonomer in ethylene/1-hexene copolymer made with different supported metallocene catalysts, crystallization temperature and crystallinity of copolymers are decreased [70]. Assumption et al. have reported that by increasing the elution temperature of ethylene/1-hexene fractions the crystallinity is enhanced [71]. Through an increase in the number of short-chain branches via the incorporation of α-olefin comonomers such as 1-butene, 1-hexene, and 1-octene, the polymer crystallinity and density can be reduced [72, 73].

By comparing the increasing trend of T_m of all the fractions (Figure 4) and also the constant values for T_c in the section (1) of Figure 6, a question is suggested that why the fractions with SCB contents lower than 7.0, show about 10 °C difference in melting temperatures while, they have very close crystallization temperatures? It should be mentioned that the MSL affects the crystallinity when the maximum MSL is less than the "critical value for the onset of chain folding", L_{crit} [59]. This means that at high SCB contents where MSL< L_{crit}, the MSL determines the crystallizability

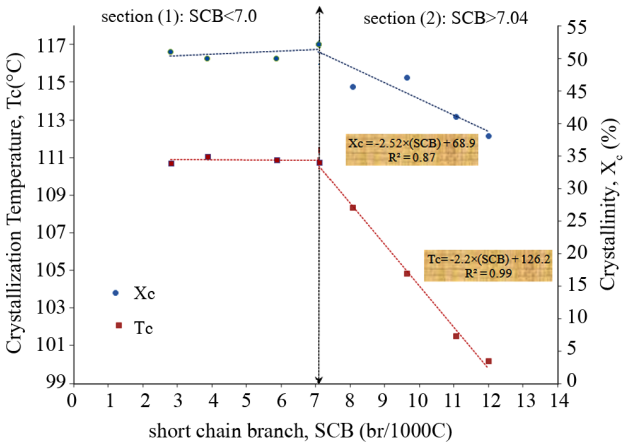

Figure 6. Tc and crystallinity versus short-chain branch content for P-TREF fractions.

of a polymer chain at given crystallization conditions. It is likely that at high SCB contents the crystallization temperature as well as the crystallinity is adjusted by the MSL or SCB content. But, at low SCB contents where MSL > L_{crit}, the crystallizability of a polymer chain at given crystallization conditions would be independent of MSL or SCB content. Although L_{crit} is reported around 250 carbons in the literature [74-76] but, it should be noted that these works have estimated L_{crit} using some linear paraffinic oligomeric calibrants such as $C_{104}H_{210}$ or uniform alkanes such as $C_{246}H_{494}$ or $C_{198}H_{398}$. Therefore, for a "polymeric" structure containing "butyl branches", the L_{crit} might be different. Based on the results obtained here, the L_{crit} for the parent polymer at the crystallization condition used here is estimated around 137 carbons (the corresponding MSL of SCB content of 7.0). Where at MSLs lower than 137 carbons, the Tc is controlled by SCB content, while at higher MSLs than 137 carbons T_c is independent of SCB content. On the other hand, melting temperature maintains its increasing trend for all fractions due to higher motivation of more linear chains.

Thermal degradation behavior: dependency on 1-hexene content

TGA/differential thermogravimetric (DTG) analysis was carried out on the parent polymer and the P-TREF fractions. The thermogravimetric data are provided in Table 4 and TGA/DTG curves are depicted in Figure 7. In order to assess the repeatability of DSC measurements, the fraction 75-80 had been consumed before TGA/DTG, and therefore, the other fractions were

Table 4. TGA/DTG data of the parent polymer and the P-TREF fractions.

Fraction	$T_{5\%}$[1] (°C)	$T_{95\%}$[2] (°C)	$T_{95\%}$- $T_{5\%}$[3] (°C)	T_{max}[4] (°C)	SCB[5] (br/1000 C)
60-70	426.1	499.1	73.0	486.5	11.9
70-75	440.6	497.6	56.9	485.4	11.0
80-85	446.8	499.0	52.3	487.1	8.1
85-90	448.8	499.1	50.3	487.4	7.0
90-95	453.8	500.8	46.9	490.2	5.8
95-100	439.4	500.4	61.0	488.8	3.8
100-110	457.1	501.1	43.9	490.1	2.7
30-140 (parent polymer)	451.9	499.2	47.4	488.2	5.8

[1] $T_{5\%}$: Temperature at 5% mass loss (degradation initiation temperature).

[2] $T_{95\%}$: Temperature at 95% mass loss (degradation termination temperature).

[3] $T_{95\%}$- $T_{5\%}$: Considered as width of DTG peak.

[4] T_{max}: Temperature at maximum degradation rate.

[5] SCB: Short-chain branch content.

tested here (Table 4).

Figures 7(a) and (b) illustrate the onset of degradation, at the temperatures of around 60°C to about 460°C, known here as "degradation initiation stage". In degradation initiation stage dissimilar behaviors are observed for different P-TREF fractions. Also, at the temperature range of around 420°C to about 520°C, a "degradation propagation stage" appears. The differences between mass loss and mass derivative curves in Figures 7 (c) and (d)) can be easily detected. As it is reflected in Table 4, by decreasing SCB content from ~12 (br/1000 C) (for fraction of 60-70°C) to ~3 (br/1000 C) (for fraction of 100-110°C) degradation initiation temperature ($T_{5\%}$) and temperature at maximum degradation rate (T_{max}) are increased moderately from ~ 426°C to ~ 457°C (3.4°C/SCB) and from ~ 487°C to ~ 490°C (0.4°C/SCB), respectively. It means that by decreasing each single SCB per 1000 carbon in the polymer backbone there would appear about 3.4°C incremental shift at $T_{5\%}$. This incremental shift changes to 0.4°C by decreasing each about single SCB per 1000 carbons in the polymer backbone at T_{max}. Based on these results, it is clearly confirmed that comono-

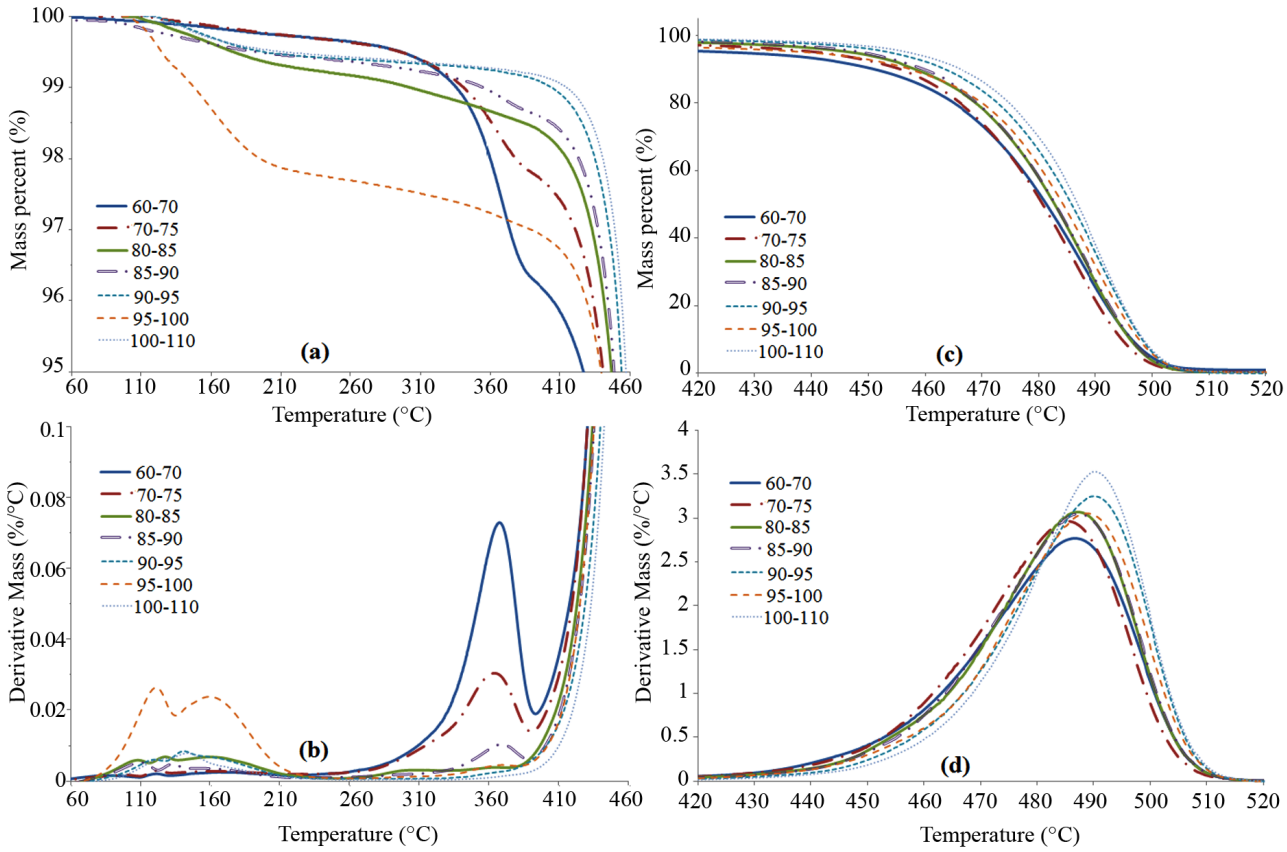

Figure 7. TGA and DTG curves of P-TREF fractions. An adapted expanded scale is used for each fraction in order to compare degradation peak shapes more accurately: (a) TGA curves of initiation stage (60-460°C), (b) DTG curves of initiation stage (60-460°C), (c) TGA curves of propagation stage (420-520°C) and (d) DTG curves of propagation stage (420-520°C).

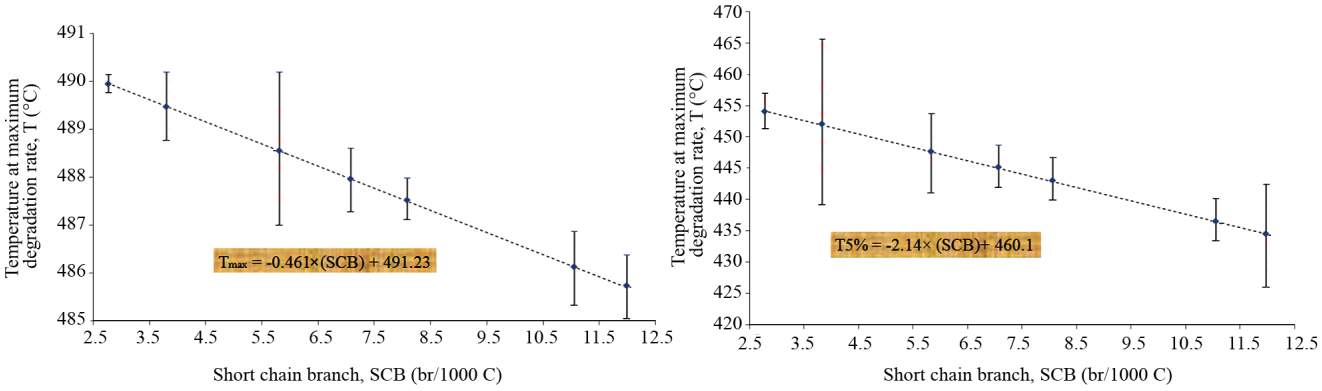

Figure 8. The trends of T_{max} (a) and $T_{5\%}$ (b) versus SCB content and the linear regressions.

mer content affects thermal degradation behavior of ethylene/1-hexene copolymer, with respect to $T_{5\%}$ and T_{max}. Also it is found that the $T_{5\%}$ is about 8.5 times more sensitive to SCB content than Tmax. Gauthier et al. have shown that MSL affects the thermo-oxidative degradation of polyethylene films [68]. As a first effort to formulate a relationship between SCB content and Tmax as well as $T_{5\%}$, Eqns 14 and 15 (Figures 8a and 8b) can be obtained using data in Table 4.

$$T_{max} = -0.46 \times (SCB) + 491.2 \quad (12)$$

$$T_{5\%} = -2.14 \times (SCB) + 460.1 \quad (13)$$

Similar values have been obtained for degradation termination temperature ($T_{95\%}$), as it is considered in Table 4. On the other hand the $T_{5\%}$ is decreased by SCB content. Therefore, it can be concluded that the width of DTG peak ($T_{95\%}$-$T_{5\%}$) is broadened by SCB content. For this reason the DTG peaks show a tail in the left side as it is visible in Figure 7(d).

CONCLUSION

The effect of comonomer content on thermal behavior (crystallization, melting and degradation) of an ethylene/1-hexene copolymer has been investigated in detail and the following findings obtained:

- A 22°C difference in Tm has been found for fractions which differ by 9 (br/1000 C) in SCB content.
- Different relationships between SCB content and physical characteristics (T_m, T_c, X_c and L_c) have been found for Phillips-based ethylene/1-hexene copolymer.
- For the first time two relationships have been obtained between thermal degradation parameters (T_{max} and $T_{5\%}$) and SCB content.
- The degradation parameters, e.g., $T_{5\%}$ and T_{max} have been observed to be decreased by comonomer content of ethylene/1-hexene copolymer.

Based on these findings it is recommended to investigate the role of other branching parameters, such as short-chain branch distribution (intermolecular and intramolecular), or short-chain branch length on low and high temperature thermal behavior of ethylene/1-hexene copolymer.

ACKNOWLEDGMENTS

We thank Dr. Hartmut Komber and Dr. Mikhail Malanin from Leibniz-Institut für Polymerforschung Dresden e.V. (IPF, Germany), for the measurements and discussions of NMR and FTIR results, respectively. We are also grateful to Petra Treppe and Dr. Albena Lederer from IPF for SEC-MALLS measurements and discussions.

REFERENCES

1. Sacchi MC, Losio S, Stagnaro P, Mancini G, Boragno L, Menichetti S, Viglianisi C, Limbo

S (2014) Macromolecular non-releasing additives for safer food packaging: application to ethylene/α-olefins and propylene based polymers. Polyolefin J 1: 1-15
2. Zohuri GH, Damavandi S, Ahmadjo S, sandaroos R, Shamekhi M (2014) Synthesis of high molecular weight polyethylene using FI catalyst. Polyolefin J 1: 25-32
3. Jeon HJ,Kim MN (2014) Degradation of linear low density polyethylene (LLDPE) exposed to UV-irradiation. Eur Polym J 52: 146-153
4. Benítez A, Sánchez JJ, Arnal ML, Müller AJ (2013) Monitoring abiotic degradation of branched polyethylenes formulated with pro-oxidants through different mechanical tests. Polyme Degrad Stabil 98: 1705-1716
5. Morlat-Therias S, Fanton E, Gardette J-L, Dintcheva NT, La Mantia FP, Malatesta V (2008) Photochemical stabilization of linear low-density polyethylene/clay nanocomposites: Towards durable nanocomposites. Polym Degard Stabil 93: 1776-1780
6. Peacock A (2000). Handbook of polyethylene: structures: properties, and applications CRC Press.
7. Ko YS, Han TK, Sadatoshi H, Woo SI (1998) Analysis of microstructure of ethylene–1-hexene copolymer prepared over thermally pretreated $MgCl_2$/THF/$TiCl_4$bimetallic catalyst. J Polym Sci Part A: Polym Chem 36: 291-300
8. Chu KJ, Soares JB, Penlidis A, Ihm SK (1999) The influence of the Ti^{3+} species on the microstructure of ethylene/1-hexene copolymers. Macromol Chem Phys 200: 1298-1305
9. Czaja K,Białek M (2001) Microstructure of ethylene-1-hexene and ethylene-1-octene copolymers obtained over Ziegler–Natta catalysts supported on MgCl2(THF)2. Polymer 42: 2289-2297
10. Van Grieken R, Carrero A, Suarez I, Paredes B (2007) Effect of 1-hexene comonomer on polyethylene particle growth and kinetic profiles. Macromol Symp 259: 243-252
11. Sarzotti DM, Soares JB, Penlidis A (2002) Ethylene/1-hexene copolymers synthesized with a single-site catalyst: Crystallization analysis fractionation, modeling, and reactivity ratio estimation. J Polym Sci Part B: Polym Phys 40: 2595-2611
12. dos Santos JHZ, Larentis A, da Rosa MB, Krug C, Baumvol IJR, Dupont J, Stedile FC, de Camargo Forte M (1999) Optimization of a silica supported bis (butylcyclopentadienyl)-zirconium dichloride catalyst for ethylene polymerization. Macromol Chem Phys 200: 751-757
13. Terano M, Soga K (1994). Catalyst Design for Tailor-Made Polyolefins, Elsevier
14. Deslauriers PJ, McDaniel MP (2007) Short chain branching profiles in polyethylene from the Phillips Cr/silica catalyst. J Polym Sci Part A: Polym Chem 45: 3135-3149
15. McDaniel MP (2010) A review of the Phillips supported chromium catalyst and its commercial use for ethylene polymerization. Adv Cat 53: 123-606
16. McDaniel M, Rohlfing D, Benham E (2003) Long chain branching in polyethylene from the Phillips chromium catalyst. Polym Reac Eng 11: 101-132
17. Tso CC, DesLauriers PJ (2004) Comparison of methods for characterizing comonomer composition in ethylene 1-olefin copolymers: 3D-TREF vs. SEC-FTIR. Polymer 45: 2657-2663
18. Shen G, Shen H, Xie B, Yang W, Yang M (2013) Crystallization and fracture behaviors of high-density polyethylene/linear low-density polyethylene blends: The influence of short-chain branching. J Appl Polym Sci 129: 2103-2111
19. Shan CLP, degroot WA, Hazlitt LG, Gillespie D (2005) A new turbidimetric approach to measuring polyethylene short chain branching distributions. Polymer 46: 11755-11767
20. Torabi S, Fazeli N (2009) A rapid quantitative method for determination of short chain branching content and branching distribution index in LLDPEs by DSC. Polym Test 28: 866-870
21. Ramachandran R, Beaucage G, McFaddin D, Merrick-Mack J, Galiatsatos V, Mirabella F (2011) Branch length distribution in TREF fractionated polyethylene. Polymer 52: 2661-2666
22. Pérez C, Alvarez V, Valles E, Failla M (2012) Crystallization behavior of random ethylene–butene copolymers modified with organic

peroxide. Thermochim Act 528: 15-22
23. He F-A,Zhang L-M (2014) Study on branching structure, melting, and crystallization of polyethylene prepared by Nickela-Diimine catalyst covalently intercalated inside oapPOSS-modified laponite clay gallery. Polym Test 35: 80-86
24. Fazeli N, Arabi H, Bolandi S (2006) Effect of branching characteristics of ethylene/1-butene copolymers on melt flow index. Polym Test 25: 28-33
25. Gupta P, Wilkes GL, Sukhadia AM, Krishnaswamy RK, Lamborn MJ, Wharry SM, Tso CC, DesLauriers PJ, Mansfield T, Beyer FL (2005) Does the length of the short chain branch affect the mechanical properties of linear low density polyethylenes? An investigation based on films of copolymers of ethylene/1-butene, ethylene/1-hexene and ethylene/1-octene synthesized by a single site metallocene catalyst. Polymer 46: 8819-8837
26. Hussein IA (2003) Influence of composition distribution and branch content on the miscibility of m-LLDPE and HDPE blends: Rheological investigation. Macromolecules 36: 2024-2031
27. Kessner U, Kaschta J, Stadler FJ, Le Duff CS, Drooghaag X, Münstedt H (2010) Thermorheological behavior of various short- and long-chain branched polyethylenes and their correlations with the molecular structure. Macromolecules 43: 7341-7350
28. Hosoda S, Nozue Y, Kawashima Y, Suita K, Seno S, Nagamatsu T, Wagener KB, Inci B, Zuluaga F, Rojas G (2010) Effect of the sequence length distribution on the lamellar crystal thickness and thickness distribution of polyethylene: perfectly equisequential ADMET polyethylene vs ethylene/α-olefin copolymer. Macromolecules 44: 313-319
29. Nitta Kh,Tanaka A (2001) Dynamic mechanical properties of metallocene catalyzed linear polyethylenes. Polymer 42: 1219-1226
30. Stadler FJ, Kaschta J, Münstedt H (2008) Thermorheological behavior of various long-chain branched polyethylenes. Macromolecules 41: 1328-1333
31. Stadler FJ, Gabriel C, Münstedt H (2007) Influence of short-chain branching of polyethylenes on the temperature dependence of rheological properties in shear. Macromol Chem Phys 208: 2449-2454
32. Carella J, Gotro J, Graessley W (1986) Thermorheological effects of long-chain branching in entangled polymer melts. Macromolecules 19: 659-667
33. Mavridis H, Shroff R (1992) Temperature dependence of polyolefin melt rheology. Polym Eng & Sci 32: 1778-1791
34. Starck P,Löfgren B (2002) Thermal properties of ethylene/long chain α-olefin copolymers produced by metallocenes. Eur Polym J 38: 97-107
35. Vanden Eynde S, Mathot V, Koch M, Reynaers H (2000) Thermal behaviour and morphology of homogeneous ethylene–propylene and ethylene–1-butene copolymers with high comonomer contents. Polymer 41: 3437-3453
36. Zhang M, Lynch D, Wanke S (2001) Effect of molecular structure distribution on melting and crystallization behavior of 1-butene/ethylene copolymers. Polymer 42: 3067-3075
37. Naddeo C, Guadagno L, De Luca S, Vittoria V, Camino G (2001) Mechanical and transport properties of irradiated linear low density polyethylene (LLDPE). Polym Degrad Stabil 72: 239-247
38. Krupa I, Luyt AS (2001) Thermal and mechanical properties of extruded LLDPE/wax blends. Polym Degrad Stabil 73: 157-161
39. Goldberg VM, Kolesnikova NN, Paverman NG, Kavun SM, Stott PE, Gelbin ME (2001) Thermo-oxidative degradation of linear low density poly(ethylene) in the presence of carbon black: a kinetic approach. Polym Degrad Stabil 74: 371-385
40. Xie R, Qu B, Hu K (2001) Dynamic FTIR studies of thermo-oxidation of expandable graphite-based halogen-free flame retardant LLDPE blends. Polym Degrad Stabil 72: 313-321
41. Wang Z, Wu G, Hu Y, Ding Y, Hu K, Fan W (2002) Thermal degradation of magnesium hydroxide and red phosphorus flame retarded polyethylene composites. Polym Degrad Stabil 77: 427-434
42. Gulmine JV, Janissek PR, Heise HM, Akcelrud L

(2003) Degradation profile of polyethylene after artificial accelerated weathering. Polym Degrad Stabil 79: 385-397
43. Naddeo C, Guadagno L, Vittoria V (2004) Photooxidation of spherilene linear low-density polyethylene films subjected to environmental weathering. 1. Changes in mechanical properties. Polym Degrad Stabil 85: 1009-1013
44. Abbas-Abadi MS, Haghighi MN, Yeganeh H (2012) The effect of temperature, catalyst, different carrier gases and stirrer on the produced transportation hydrocarbons of LLDPE degradation in a stirred reactor. J Anal Appl Pyro 95: 198-204
45. Gascoin N, Fau G, Gillard P, Mangeot A (2013) Experimental flash pyrolysis of high density polyethylene under hybrid propulsion conditions. J Anal Appl Pyro 101: 45-52
46. Arabiourrutia M, Elordi G, Lopez G, Borsella E, Bilbao J, Olazar M (2012) Characterization of the waxes obtained by the pyrolysis of polyolefin plastics in a conical spouted bed reactor. J Anal Appl Pyro 94: 230-237
47. Murata K, Brebu M, Sakata Y (2010) The effect of silica–alumina catalysts on degradation of polyolefins by a continuous flow reactor. J Anal Appl Pyro 89: 30-38
48. De Stefanis A, Cafarelli P, Gallese F, Borsella E, Nana A, Perez G (2013) Catalytic pyrolysis of polyethylene: A comparison between pillared and restructured clays. J Anal Appl Pyro 104: 479-484
49. Singhal R, Singhal C, Upadhyayula S (2010) Thermal-catalytic degradation of polyethylene over silicoaluminophosphate molecular sieves-A thermogravimetric study. J Anal Appl Pyro 89: 313-317
50. Renzini MS, Lerici LC, Sedran U, Pierella LB (2011) Stability of ZSM-11 and BETA zeolites during the catalytic cracking of low-density polyethylene. J Anal Appl Pyro 92: 450-455
51. He P, Xiao Y, Zhang P, Xing C, Zhu N, Zhu X, Yan D (2005) Thermal degradation of syndiotactic polypropylene and the influence of stereoregularity on the thermal degradation behaviour by in situ FTIR spectroscopy. Polymer Degrad Stabil 88: 473-479
52. Westerhout R, Waanders J, Kuipers J, Van Swaaij W (1997) Kinetics of the low-temperature pyrolysis of polyethene, polypropene, and polystyrene modeling, experimental determination, and comparison with literature models and data. Ind Eng Chem Res 36: 1955-1964
53. Abbas-Abadi MS, Haghighi MN, Yeganeh H (2013) Evaluation of pyrolysis product of virgin high density polyethylene degradation using different process parameters in a stirred reactor. Fuel Process Technol 109: 90-95
54. Abbas-Abadi MS, Haghighi MN, Yeganeh H, Bozorgi B (2013) The effect of melt flow index, melt flow rate, and particle size on the thermal degradation of commercial high density polyethylene powder. J Therm Anal ad Calor 114: 1333-1339
55. Kebritchi A, Nekoomanesh H. M, Mohammadi F, Khonakdar HA (submitted) The interrelationship of microstructure and low/high temperature thermal behavior of fractionated ethylene/1-butene copolymer. Iran. Polym. J
56. Fu Y,Lim L-T (2012) Investigation of multiple-component diffusion through LLDPE film using an FTIR-ATR technique. Polym Test 31: 56-67
57. Kim YM,Park JK (1996) Effect of short chain branching on the blown film properties of linear low density polyethylene. J Appl Polym Sci 61: 2315-2324
58. Defoor F, Groeninckx G, Schouterden P, Van der Heijden B (1992) Molecular, thermal and morphological characterization of narrowly branched fractions of 1-octene linear low-density polyethylene: 1. molecular and thermal characterization. Polymer 33: 3878-3883
59. Zhang M, Wanke SE (2003) Quantitative determination of short-chain branching content and distribution in commercial polyethylenes by thermally fractionated differential scanning calorimetry. Polym Eng Sci 43: 1878-1888
60. Kakugo M, Miyatake T, Mizunuma K (1991) Chemical composition distribution of ethylene-1-hexene copolymer prepared with titanium trichloride-diethylaluminum chloride catalyst. Macromolecules 24: 1469-1472
61. Adisson E, Ribeiro M, Deffieux A, Fontanille

M (1992) Evaluation of the heterogeneity in linear low-density polyethylene comonomer unit distribution by differential scanning calorimetry characterization of thermally treated samples. Polymer 33: 4337-4342

62. Hosoda S (1988) Structural distribution of linear low-density polyethylenes. Polymer J 20: 383-397
63. Shanks R, Amarasinghe G (2000) Comonomer distribution in polyethylenes analysed by DSC after thermal fractionation. J Thermal Anal Calorimetry 59: 471-482
64. Yoon J-S, Lee D-H, Park E-S, Lee I-M, Park D-K, Jung S-O (2000) Thermal and mechanical properties of ethylene/α-olefin copolymers produced over $(2\text{-MeInd})_2ZrCl_2$/MAO system. Polymer 41: 4523-4530
65. Teng H, Shi Y, Jin X (2002) Novel characterization of the crystalline segment distribution and its effect on the crystallization of branched polyethylene by differential scanning calorimetry. J Polym Sci Part B: Polym Phys 40: 2107-2118
66. Fan Z, Wang Y, Bu H (2003) Influence of intermolecular entanglements on crystallization behavior of ultra-high molar mass polyethylene. Polym Eng Sci 43: 607-614
67. Mortazavi SMM, Arabi H, Zohuri G, Ahmadjo S, Nekoomanesh M, Ahmadi M (2010) Copolymerization of ethylene/α-olefins using bis(2-phenylindenyl)zirconium dichloride metallocene catalyst: structural study of comonomer distribution. Polym Int 59: 1258-1265
68. E. Gauthier BL, F.J.J.M. Cuoq, P.J. Halley, K.A. George (2012) Correlation between chain microstructural changes and embrittlement of LLDPE-based films during photo- and thermo-oxidative degradation. Polym Degrad Stabil: 1-12
69. Pérez CJ, Failla M, Carella J (2013) SSA study of early polyethylenes degradation stages. Effects of attack rate, of average branch length, and of backbone polymethylene sequences length distributions. Polym Degrad Stabil 98: 177-183
70. Paredes B, Soares JB, van Grieken R, Carrero A, Suarez I (2007) Characterization of ethylene-1-Hexene copolymers made with supported metallocene catalysts: influence of support type. Macromol Symp 257: 103-111
71. Assumption H, Vermeulen J, Jarrett WL, Mathias LJ, Van Reenen A (2006) High resolution solution and solid state NMR characterization of ethylene/1-butene and ethylene/1-hexene copolymers fractionated by preparative temperature rising elution fractionation. Polymer 47: 67-74
72. Simanke A, Galland G, Baumhardt Neto R, Quijada R, Mauler R (1999) Influence of the type and the comonomer contents on the mechanical behavior of ethylene/α-olefin copolymers. J Appl Polym Sci 74: 1194-1200
73. Kale L, Plumley T, Patel R, Redwine O, Jain P (1996) Structure-property relationships of ethylene/1-octene and ethylene/1-butene copolymers made using INSITE technology. J Plast film Sheet 12: 27-40
74. Bonner J, Frye C, Capaccio G (1993) A novel calibration for the characterization of polyethylene copolymers by temperature rising elution fractionation. Polymer 34: 3532-3534
75. Ungar G, Keller A (1987) Inversion of the temperature dependence of crystallization rates due to onset of chain folding. Polymer 28: 1899-1907
76. Stack GM, Mandelkern L (1988) On the crystallization of high molecular weight normal hydrocarbons. Macromolecules 21: 510-514